Applied Surface Science 390 (2016) 283–288

Contents lists available at ScienceDirect

Applied Surface Science

journal homepage: www.elsevier.com/locate/apsusc

Study of the helium cross-section of unsymmetric disulfide self-assembled monolayers on Au(111)

Erol Albayrak[a], Semistan Karabuga[b], Gianangelo Bracco[c], M. Fatih Danışman[d,*]

[a] Department of Materials and Metallurgical Engineering, Ahi Evran University, Kırşehir 40000, Turkey
[b] Department of Chemistry, Kahramanmaraş Sütçü İmam University, Kahramanmaraş 46030, Turkey
[c] CNR-IMEM and Department of Physics, University of Genoa, Via Dodecaneso 33, Genoa 16146, Italy
[d] Department of Chemistry, Middle East Technical University, Ankara 06800, Turkey

ARTICLE INFO

Article history:
Received 25 May 2016
Received in revised form 28 July 2016
Accepted 11 August 2016
Available online 17 August 2016

Keywords:
Self-assembled monolayers
Unsymmetric disulfides
The scattering cross sections
Supersonic molecular beam deposition
11-Hydroxyundecyl decyl disulfide
11-Hydroxyundecyl octadecyl disulfide

ABSTRACT

We have investigated the formation of self-assembled monolayers (SAMs) of 11-hydroxyundecyl decyl disulfide (CH_3-$(CH_2)_9$-S-S-$(CH_2)_{11}$-OH, HDD) and 11-hydroxyundecyl octadecyl disulfide (CH_3-$(CH_2)_{17}$-S-S-$(CH_2)_{11}$-OH, HOD) produced by supersonic molecular beam deposition (SMBD). The study has been carried out by means of helium diffraction at very low film coverage. In this regime helium single molecule cross sections have been estimated in a temperature range between 100 K and 450 K. The results show a different behavior above 300 K that has been interpreted as the starting of mobility with the formation of two thiolate moieties either linked by a gold adatom or distant enough to prevent cross section overlapping. Finally, helium diffraction patterns measured at 80 K for the SAMs grown at 200 K are discussed and the results support the proposed hypothesis of molecular dissociation based on the cross section data.

1. Introduction

Self-assembled monolayers (SAMs) of disulfides have found use in formation of mixed SAMs that can be utilized in nanotechnological applications like controlled protein adsorption [1,2] or polymer growth on a surface. [3] In the past they have been studied extensively in order to understand the formation mechanism of thiolate films on Au(111) surfaces [4–6]. By using unsymmetric disulfides (R-S-S-R', will be referred to UDS) and investigating the phase separation of different thiolates on the surface it was possible to derive conclusions regarding the occurring/mechanism of S—S bond cleavage [7–11].

Currently it is well established that, whether prepared from thiols (R-S-H) or symmetric disuldifes (R-S-S-R), the full coverage thiolate SAMs (where the molecules stand up and pack densely) form a $(\sqrt{3} \times \sqrt{3})R30^\circ$ structure. Many experimental and theoretical investigations have been performed in order to understand the details of this structure (such as an adsorption site of the sulfur atoms). Currently the most accepted model includes formation thiolate-Au adatom-thiolate (RS-Au_{ad}-SR) dimers [12–16]. At low coverage, on the other hand, the molecules lie parallel to the surface and form the so called striped phases [4–6]. However, when unsymmetric disulfides were employed, to investigate S—S bond cleavage, contradictory results were obtained. In case of full coverage SAMs of CH_3-$(CH_2)_m$-S-S-$(CH_2)_n$-OH no phase separation was observed by several research groups. [17–19] On the other hand for low coverage UDS films there are very few studies[9–11] and for m = 17 and n = 11 phase separation was observed which was evidenced by the formation of two different corrugation periodicities consistent with the lengths of separated thiolates. [10]

We recently performed a helium scattering study of 11-hydroxyundecyl decyl disulfide (CH_3-$(CH_2)_9$-S-S-$(CH_2)_{11}$-OH, HDD) and 11-hydroxyundecyl octadecyl disulfide (CH_3-$(CH_2)_{17}$-S-S-$(CH_2)_{11}$-OH, HOD) SAMs grown in vacuum by means of supersonic molecular beam deposition (SMBD) [20,21]. Using helium scattering and SMBD allowed us to study the film growth at low coverage very precisely, due to the very sensitive nature of helium scattering to surface corrugation caused by the long range interaction of the helium atoms with the surface. In the past this property of helium scattering was exploited for very precise monitoring of the coverage of organic and inorganic films on metal surfaces. [20–33] For instance Comsa and co-workers studied CO adsorption on metal surfaces and proposed several models to correlate helium specular reflection intensity to film coverage [33]. Based on these models they were able to extract scattering

* Corresponding author.
E-mail address: danisman@metu.edu.tr (M.F. Danışman).

http://dx.doi.org/10.1016/j.apsusc.2016.08.062
0169-4332/

cross section values of CO molecules. They were also able to detect migration of adsorbates to steps and step saturation by monitoring specular reflection intensity at different substrate temperatures [34]. In addition, conclusions regarding the adsorption mechanism of the molecules can be reached by analyzing the specular reflection and estimating the helium scattering cross section of the adsorbed species. To this end here we focused on the very early stage of the HDD and HOD film formation in order to calculate the scattering cross sections for isolated lying down molecules. We have analyzed data which were already presented in References [20] and [21] but couldn't have been discussed from the point of view relevant to this article as well as new data measured to complete the present work. In addition, we provide detailed diffraction data for the low temperature lying down monolayer phase of these UDS SAMs to further support the proposed dissociation hypothesis based on the cross section calculations.

2. Experimental

The experimental setup was extensively described before [35,36] and here we give only a brief description relevant to the present study. Thiol films were grown by using a supersonic molecular beam deposition source whose temperature determines the flux of thiol molecules during deposition. Reasonable HDD and HOD flux values were achieved at source temperatures of 130–145 °C and 160–180 °C respectively. Characterization of the films was performed by using a helium beam produced by a source working at about 70 K. The Au(111) surface with an orientation accuracy of <0.1° was purchased from Mateck GmbH. Before deposition experiments the gold surface was treated with several sputter-anneal cycles and the cleanness was confirmed by observation of the gold reconstruction diffraction peaks and a specular reflection intensity greater than 25% of the incident beam. In consecutive depositions, after high temperature anneal to desorb/remove completely the thiol film, the fulfillment of this observation was also employed to assess cleanness before to grow a new film. In case of HDD, four separate depositions experiments were performed at 200 K and two deposition experiments were performed at 265 K, 300 K and 350 K. For the remaining temperatures for HDD and for all the temperatures for HOD only one deposition measurement was performed. HDD and HOD were synthesized by following the procedure proposed by Flores et al. [19] and a detailed procedure is described in our previous reports. [20,21]

3. Results

In Fig. 1 we show deposition curves for HDD and HOD films, i.e. helium specular reflection (SR) intensity normalized to the intensity of the bare substrate as a function of film coverage, for different deposition rates (panel (a)) and for different substrate temperatures (panels (b) and (c)). As film coverage increases, SR intensity decreases due to increasing surface roughness. As the first monolayer (ML) completes however a relatively smoother surface forms that result in a partial recovery of the SR intensity. Here we should note that by ML we refer to full monolayer lying down striped phase but not the high density standing up monolayer phase. After completion of the ML, further adsorption, again, increases the surface roughness till it reaches a steady state resulting in a constant low SR intensity signal. As can be seen in panel (a) of Fig. 1 even at fixed temperature, different deposition curves do not exactly overlap and the difference does not seem to be correlated to the deposition rate. Throughout the deposition measurements reported here we tried to keep the deposition rate R in the range of R^{-1} = 100–300 s/ML but for some HOD depositions a drift in the deposition source conditions produced an inverse rate as low as 700 s/ML. Here we will focus on the initial parts of deposition curves, specifically from 0 to

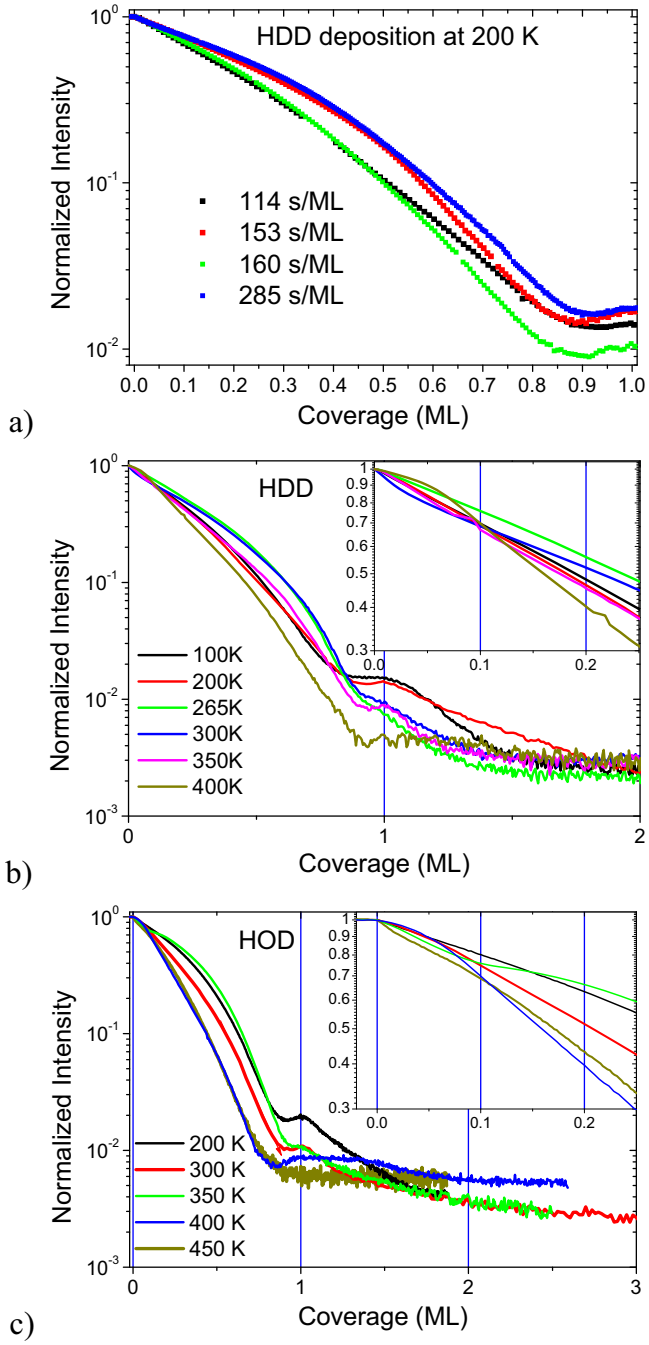

Fig. 1. Deposition curves showing helium specular reflection intensity as a function of HDD (a, b) and HOD (c) coverage on Au(111) for different deposition rates (a) and at different substrate temperatures (b, c).

0.25 ML region which are shown in the insets of Fig. 1. These initial parts of the deposition curves are used to estimate the molecular cross-section of the adsorbing molecules. To this end, two different models proposed by Comsa [33] have been used: "fully random" and "maximum repulsion". In the "fully random" model molecules are assumed to adsorb randomly on the surface and the change in the helium SR intensity, I, can be related to the coverage, θ, of the adsorbing molecules as follows:

$$\frac{I}{I_0} = e^{-\theta n_s \Sigma}$$

Where I_0 is the SR intensity at zero coverage, n_s is the number of the substrate atoms per unit area (which is 0.139 Å^{-2} for Au(111))

and Σ is the scattering cross-section (cs). We should note here that definition of coverage, θ, used in this model is different from the definition used in Figs. 1 and 2 and corresponds to the ratio of number of adsorbed molecules per unit area, n, to n_s. Hence 1 ML coverage indicated in Figs. 1 and 2 corresponds to a θ value of 0.044 (with $n = 6.09 \times 10^{-3}$ Å^{-2}) for HDD and 0.034 (with $n = 4.66 \times 10^{-3}$ Å^{-2}) for HOD. In the "maximum repulsion" model, where the molecules are assumed to stay as far away from each other as possible, the above formula is modified as follows:

$$\frac{I}{I_0} = 1 - \theta n_s \Sigma$$

A full quantum mechanical calculation of the cross section performed on realistic interaction potentials is beyond the aim of the present article and a phenomenological approach will be given that is useful to extract information from the data. A pure geometrical estimation of the cs may rely on the Van der Waals (vdW) radius of all the atoms which are forming HDD and HOD molecules in their all-trans forms. At semi empirical (AM1) level the dimensions of the molecules (distance between the hydrogen nuclei at the peripheries) can be calculated to be (31.0 Å × 2.2 Å) and (41.1 Å × 2.2 Å) respectively. By adding the vdW radius of hydrogen atom (1.2 Å) to these values the vdW dimensions of the molecules can be estimated to be (33.4 Å × 4.6 Å) and (43.5 Å × 4.6 Å) with the corresponding cs (cs_{vdW}) values of 154 Å^2 and 200 Å^2 respectively. On the other hand the effective cross section cs_e should take into account the finite size of the He probe (vdW radius 1.4 Å) increasing the molecular dimension to (36.2 Å × 7.4 Å) and (46.3 Å × 7.4 Å) and the vdW cs to 268 Å^2 and 343 Å^2 respectively. Analyzing the results for simple molecules we observe that Comsa and coworkers reported the He scattering cross section radius of CO molecules to be 6 Å more than their hard sphere radius. [32,33] Adding this 6 Å region to the vdW

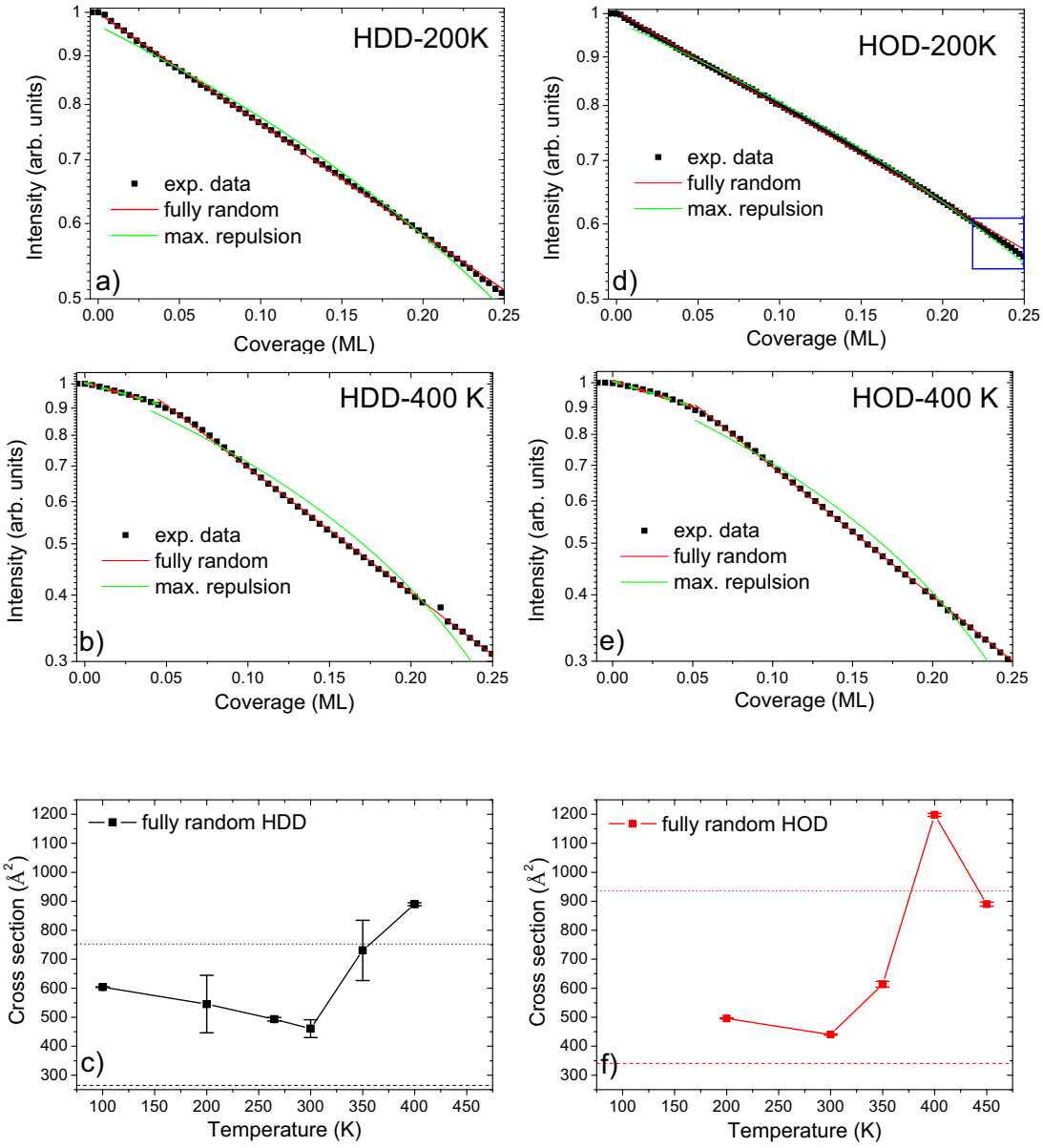

Fig. 2. Deposition curves for (a) HDD at 200 K, (b) HDD at 400 K, (d) HOD at 200 K and (e) HOD at 400 K. Black curves show experimental data while the colored curves are fit results. Scattering cross sections as a function of deposition substrate temperature, deduced from the fit results are plotted in (c) and (f). The cs_e and cs_{max} values are indicated by dashed and dotted lines respectively in (c) and (f). The reported cs values in (c) and (f) for high substrate temperatures were extracted from the 0.05–0.25 ML region of the deposition curves as discussed in the text. In part (f) the cs value at 350 K was extracted from the 0–0.1 ML region of the corresponding deposition curve (green trace in Fig. 1c). (For interpretation of the references to colour in this figure legend, the reader is referred to the web version of this article.)

dimensions of the HDD and HOD molecules their effective cross section can be calculated to be as high as 754 Å^2 (45.4 Å × 16.6 Å) and 921 Å^2 (55.5 Å × 16.6 Å) respectively (cs values calculated with this additional 6 Å region will be referred to as cs_{max}). Of course, these are only indicative values estimated by starting with rigid vdW spheres. On the other hand, these values are useful to draw direct conclusions as it will be discussed in the following sections.

Fitting results obtained with "fully random" and "maximum repulsion" models for two set of representative deposition curves are reported in Fig. 2. In general, the exponential behavior of "fully random" model resulted in a better fit than the linear decay of the "maximum repulsion" model, especially more so for high substrate temperatures, which indicate that the molecules adsorb randomly on the surface. The standard error of each fit was no more than ±10 Å^2 in case of "fully random" model.

Curves in panels a) and d) of Fig. 2 are qualitatively different from those in panels b) and e). For substrate temperatures lower than 300 K the deposition curves in logarithmic scale present an almost linear decay and can be fitted by a single function. Instead at higher temperatures, two different regions with different slopes are present and the points show a change of the slope for very small coverage around 0.05 ML. This behavior is similar to what was observed for the deposition on stepped surfaces [34,37] and the first part of the curve (from 0 to 0.05 ML) can be associated to the adsorption at step edges and the second part with a higher slope (from 0.05 to 0.25 ML) to adsorption onto terraces. The initial slow decay region can be fitted by "fully random" and "maximum repulsion" models equally well (as shown with dashed lines in Fig. 2b, e) and the resulting cs are only slightly larger than the cs_{vdW} of the molecules (for instance, the calculated "fully random" cross section estimated from the initial slow decay part of the curve shown in Fig. 2b is 332 Å^2. On the other hand, the molecular cs might be modified by the presence of the step edge and very likely by the overlap with the step edge's own cs.).

Instead, the cs calculated for the second region (0.05–0.25 ML) are much larger and the fit is very poor with "maximum repulsion" model (see solid lines in Fig. 2.b, e). Hence we believe the adsorption takes place randomly and below we will discuss only the "fully random" fit results. Evolution of the ("fully random") cs as a function of substrate temperature is summarized in Fig. 2.c and f where for high substrate temperature films the fit results obtained from the second region (0.05–0.25 ML) were plotted. The error bars reported in Fig. 2.c and f are either standard deviation values of the averages in case more than one measurement was performed or simply the standard error of the fit in case only one measurement was performed at the given temperature. Though there is significant uncertainty in the cs values for HDD at 200 K and 350 K, the evolution of cs as a function of substrate temperature can still be interpreted as follows:

Since the Au sample is the same for all the measurements and hence the average step density is the same for all the sample preparations, the observation of adsorption at steps for higher temperature suggests that below 300 K the mobility of molecules is very low, the molecules stick where they land and cannot reach a step. For higher temperatures, the cross section values reported in Fig. 2c and f suggest that the molecules are dissociated and it is reasonable to assume the mobility of the lighter and smaller fragments is higher than not dissociated molecules. In case of the dissociated molecules the effective cross-section for each dissociated disulfide can be approximated as the combination of the separate cross-sections of two thiolate groups that make up the molecule. cs_{max} values of hydroxyundecylthiolate (MUD), decanethiolate (DT) and octadecanethiolate (ODT) can be calculated as 500 Å^2, 464 Å^2 and 630 Å^2 respectively. Hence, if the thiolate groups are far from each other after dissociation (that is no overlap of cs) the cs_{max} of a dissociated disulfide will simply be equal to the sum of the separate thiolate cs_{max} which can be calculated as 964 Å^2 and 1130 Å^2 respectively for HDD and HOD. Another possibility may be the formation of RS-Au_{ad}-SR' dimers which have been reported to form at high coverage [12,13]. In case of HDD deposition, the possible dimers that can form are DT-Au_{ad}-MUD, DT-Au_{ad}-DT, MUD-Au_{ad}-MUD which have cs_{max} values of 809 Å^2, 772 Å^2 and 845 Å^2 respectively. In case of HOD deposition the possible dimers that can form are ODT-Au_{ad}-MUD, ODT-Au_{ad}-ODT, MUD-Au_{ad}-MUD which have cs_{max} values of 974 Å^2, 1104 Å^2 and 845 Å^2 respectively. We can observe that for truly isolated (far apart) molecules the first values corresponding to unsymmetric dimers are the only possible ones but in presence of mobility and for higher coverages also the formation of symmetrical dimers can become probable.

The ("fully random") cs results, summarized in Fig. 2c and f, clearly show that above 350 K the measured cs values are greater than the estimated cs_{max} for dissociated molecules or for RS-Au_{ad}-SR' dimers supporting the idea that the two thiolate groups are separated. At 300 K the cs values take their minimum value therefore He atoms see the disulfide molecules as more compact. This strange trend is likely related to the dissociation since it is hard to believe that the non-dissociated molecules could shrink (at temperatures lower than 300 K). In fact, without the constraint of the disulfide bond, the thiolate groups may pack more efficiently reducing the cs. Increasing the temperature, the thiolate groups start to migrate but, if they are not far from each other, scattering helium atoms can still see a single molecular entity, i.e. there is some overlap of thiolate cross sections therefore the cs value will increase from the minimum value to a maximum value until each thiolate will be enough separated by the other one and the cs value should tend to the sum of the two effective cross sections of single thiolate groups. One other point that needs to be addressed here is the decrease in the cs of HOD at 450 K. It has been shown that desorption of thiolates from the gold surface starts after 400 K reaching the maximum rate slightly above 450 K. [29,38] Desorption may be in the form thiol (R-S-H), thiolate (R-S) or dissociated hydrocarbon chain (R). [39–41] In addition it was shown that after 350 K concentration of gauche defects in the film increases considerably. [42] Hence we believe at 450 K molecules have enough energy to stand up and/or to adopt folded configurations which can decrease the cs significantly. Finally, we should also mention that with increasing coverage a cross-over between "fully random" adsorption and "maximum repulsion" may also be possible. In fact, when Fig. 2.d is examined (see blue rectangle) it can be seen that for coverages above 0.21 ML the data start to slightly deviate from the exponential behavior with a higher decay. In Fig. 1 increase of the decay for coverages higher than ~0.4 ML can be easily seen and this trend can be explained by the closer distance of molecules that start to interact with each other.

Based on the cs values discussed above we conclude that at 200 K disulfides adsorb on the surface as a whole and fragment separation occurs after annealing above 250 K. In fact, structural and thermal properties of the low temperature lying down ML phases which will be detailed below support this hypothesis. In Refs. [20] and [21] we had shown that for both HOD and HDD the lying down monolayer film structure is different for deposition temperatures of 200 K and 300 K with the 200 K structure [will be referred to as low temperature (LT) phase] transforming irreversibly to that observed at 300 K [will be referred to as high temperature (HT) phase] upon annealing to 300 K. What is surprising is that for both HOD and HDD the LT phases have identical diffractions patterns which are shown in Fig. 3. It can clearly be seen in this figure that the overall structure and the diffraction peak positions for the two SAMs are the same. Though we recorded diffraction scans of this LT phase along different azimuthal directions (as shown in Fig. 4) we were not able to derive a definite conclusion regarding the unit

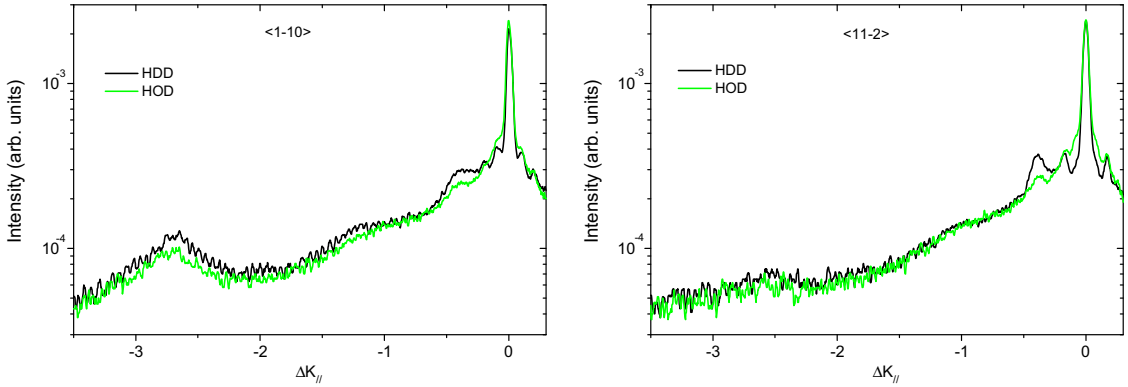

Fig. 3. Comparison of diffraction scans of HDD and HOD MLs grown at 200 K substrate temperature.

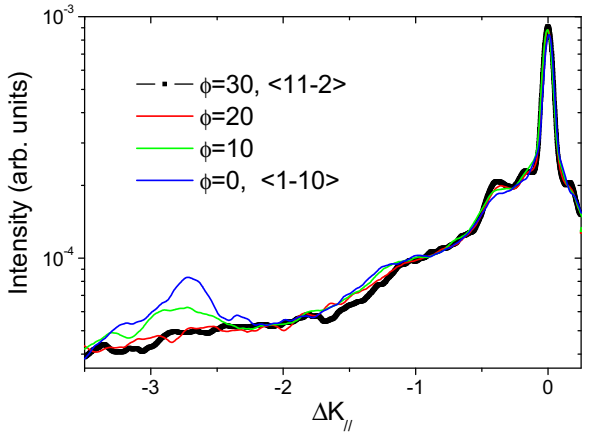

Fig. 4. Diffraction scans of HDD ML grown at 200 K substrate temperature along different crystallographic directions. ⟨1–10⟩ direction is assigned 0° azimuthal angle and the data are smoothed by adjacent point averaging for clarity.

cell structure based on this (poor) data. While we believe the identical unit cell structures are dictated by the S—S bonds, at this point we are not able to propose a reliable model that can explain how two different molecules with a large size difference can assume the same unit cell structure. Nevertheless, observation of a common LT phase for both disulfides which irreversibly transforms into a HT phase upon annealing may be considered as a further proof of the hypothesis discussed above regarding S—S bond dissociation above 250 K.

4. Discussion and conclusion

Here we have studied the evolution of the helium scattering cross sections of HOD and HDD molecules on Au(111) surface with changing temperature. The fact that below 300 K measured cs values are intermediate between cs_e and cs_{max} indicates that in this temperature range S—S bonds (disulfides) are either intact or, even if cleaved, the fragments have a small distance to each other to preserve the cross section and in turn a small S—S distance. Above 300 K however cs values increase with temperature reaching a maximum value (even higher than cs_{max}) at 400 K which we believe to be due to S—S bond cleavage that is followed by diffusion of the thiolates on the surface which may also yield to RS-Au_{ad}-SR' dimer formation. The diffusion of molecules at high temperature (T >300 K) is also supported by the qualitatively different behavior of the deposition curves: at high temperature two slopes are present and the very initial part is related to diffusion to step.

This dissociation hypothesis is in agreement with the XPS studies on dimethyldisulfide SAMs which report adsorption as disulfide at low temperature and S-S bond cleavage upon annealing to 250 K [43] In addition our recent He diffraction measurements [20,21] and scanning tunneling microscopy studies by other research groups [10] about the striped phases of unsymmetric disulfides are also in agreement with a mechanism that involves bond cleavage and phase separation at room temperature. The fact that, based on the cs values, He diffraction measurements can provide information regarding the average distance between thiolate fragments on the surface, which is not possible by XPS measurements, makes He diffraction a complementary tool to XPS. The identical crystal structures of HDD and HOD films at low temperature (200 K) however is puzzling and needs further investigation.

Acknowledgment

This work was supported by The Scientific and Technological Research Council of Turkey, TÜBİTAK, Grant No. 209T084.

References

[1] Z. Matharu, A.J. Bandodkar, V. Gupta, B.D. Malhotra, Fundamentals and application of ordered molecular assemblies to affinity biosensing, Chem. Soc. Rev. 41 (2012) 1363–1402.
[2] P. Thevenot, W.J. Hu, L.P. Tang, Surface chemistry influences implant biocompatibility, Curr. Top. Med. Chem. 8 (2008) 270–280.
[3] J.E. Raynor, J.R. Capadona, D.M. Collard, T.A. Petrie, A.J. Garcia, Polymer brushes and self-assembled monolayers: versatile platforms to control cell adhesion to biomaterials (review), Biointerphases 4 (2009) FA3–FA16.
[4] F. Schreiber, Structure and growth of self-assembling monolayers, Prog. Surf. Sci. 65 (2000) 151–256.
[5] J.C. Love, L.A. Estroff, J.K. Kriebel, R.G. Nuzzo, G.M. Whitesides, Self-assembled monolayers of thiolates on metals as a form of nanotechnology, Chem. Rev. 105 (2005) 1103–1169.
[6] C. Vericat, M.E. Vela, G. Corthey, E. Pensa, E. Cortes, M.H. Fonticelli, F. Ibanez, G.E. Benitez, P. Carro, R.C. Salvarezza, Self-assembled monolayers of thiolates on metals: a review article on sulfur-metal chemistry and surface structures, RSC Adv. 4 (2014) 27730–27754.
[7] T. Ishida, S. Yamamoto, W. Mizutani, M. Motomatsu, H. Tokumoto, H. Hokari, H. Azehara, M. Fujihira, Evidence for cleavage of disulfides in the self-assembled monolayer on Au(111), Langmuir 13 (1997) 3261–3265.
[8] M.W. Tsao, J.F. Rabolt, H. Schonherr, D.G. Castner, Semifluorinated/hydrogenated alkylthiol thin films: a comparison between disulfides and thiol binary mixtures, Langmuir 16 (2000) 1734–1743.
[9] J.G. Noh, Nano-identification for the cleavage of disulfide bond during the self-assembly processes of unsymmetric dialkyl disulfides on Au(111), Bull. Korean Chem. Soc. 26 (2005) 553–557.
[10] J. Noh, M. Hara, Nanoscopic evidence for dissociative adsorption of asymmetric disulfide self-assembled monolayers on Au(111), Langmuir 16 (2000) 2045–2048.
[11] J. Noh, T. Murase, K. Nakajima, H. Lee, M. Hara, Nanoscopic investigation of the self-assembly processes of dialkyl disulfides and dialkyl sulfides on Au(111), J. Phys. Chem. B 104 (2000) 7411–7416.

[12] R. Mazzarello, A. Cossaro, A. Verdini, R. Rousseau, L. Casalis, M.F. Danisman, L. Floreano, S. Scandolo, A. Morgante, G. Scoles, Structure of a CH3S monolayer on Au(111) solved by the interplay between molecular dynamics calculations and diffraction measurements, Phys. Rev. Lett. 98 (2007).
[13] A. Cossaro, R. Mazzarello, R. Rousseau, L. Casalis, A. Verdini, A. Kohlmeyer, L. Floreano, S. Scandolo, A. Morgante, M.L. Klein, G. Scoles, X-ray diffraction and computation yield the structure of alkanethiols on gold(111), Science 321 (2008) 943–946.
[14] L. Ferrighi, Y.X. Pan, H. Gronbeck, B. Hammer, Study of alkylthiolate self-assembled monolayers on Au(111) using a semilocal meta-GGA density functional, J. Phys. Chem. C 116 (2012) 7374–7379.
[15] D. Otalvaro, T. Veening, G. Brocks, Self-assembled monolayer induced Au(111) and Ag(111) reconstructions: work functions and interface dipole formation, J. Phys. Chem. C 116 (2012) 7826–7837.
[16] P. Carro, X. Torrelles, R.C. Salvarezza, A novel model for the (root 3 × root 3)R30 degrees alkanethiolate-Au(111) phase based on alkanethiolate-Au adatom complexes, Phys. Chem. Chem. Phys. 16 (2014) 19017–19023.
[17] T. Takami, E. Delamarche, B. Michel, C. Gerber, H. Wolf, H. Ringsdorf, Recognition of individual tail groups in self-assembled monolayers, Langmuir 11 (1995) 3876–3881.
[18] S.F. Chen, L.Y. Li, C.L. Boozer, S.Y. Jiang, Controlled chemical and structural properties of mixed self-assembled monolayers by coadsorption of symmetric and asymmetric disulfides on Au(111), J. Phys. Chem. B 105 (2001) 2975–2980.
[19] S.M. Flores, A. Shaporenko, C. Vavilala, H.J. Butt, M. Schmittel, M. Zharnikov, R. Berger, Control of surface properties of self-assembled monolayers by tuning the degree of molecular asymmetry, Surf. Sci. 600 (2006) 2847–2856.
[20] E. Albayrak, S. Karabuga, G. Bracco, M.F. Danisman, Investigation of the deposition and thermal behavior of striped phases of unsymmetric disulfide self-assembled monolayers on Au(111): the case of 11-hydroxyundecyl decyl disulfide, J. Chem. Phys. 142 (2015).
[21] E. Albayrak, S. Karabuga, G. Bracco, M.F. Danisman, 11-Hydroxyundecyl octadecyl disulfide self-assembled monolayers on Au(111), Appl. Surf. Sci. 311 (2014) 643–647.
[22] B. Poelsema, S.T. Dezwart, G. Comsa, Scattering cross-section of low-coverage co on Pt(III) for thermal He and H-2 beams, Phys. Rev. Lett. 49 (1982) 578–581.
[23] R. Kunkel, B. Poelsema, L.K. Verheij, G. Comsa, Reentrant layer-by-layer growth during molecular-beam epitaxy of metal-on-metal substrates, Phys. Rev. Lett. 65 (1990) 733–736.
[24] J. Oh, T. Kondo, D. Hatake, K. Arakawa, T. Suzuki, D. Sekiba, J. Nakamura, Adsorption of CO on iron clusters on graphite, J. Phys. Chem. C 116 (2012) 7741–7747.
[25] J. Oh, T. Kondo, D. Hatake, Y. Honma, K. Arakawa, T. Machida, J. Nakamura, He and Ar beam scatterings from bare and defect induced graphite surfaces, J. Phys-Condens. Matter 22 (2010).
[26] J.J. de Miguel, J. Camarero, R. Miranda, Studies of surface diffusion and growth on Cu(111) by means of thermal energy atom scattering, J. Phys.-Condens. Matter 14 (2002) 6155–6172.
[27] P. Schwartz, F. Schreiber, P. Eisenberger, G. Scoles, Growth kinetics of decanethiol monolayers self-assembled on Au(111) by molecular beam deposition: an atomic beam diffraction study, Surf. Sci. 423 (1999) 208–224.
[28] N. Camillone, T.Y.B. Leung, G. Scoles, A low energy helium atom diffraction study of decanethiol self-assembled on Au(111), Surf. Sci. 373 (1997) 333–349.
[29] M.F. Danisman, L. Casalis, G. Bracco, G. Scoles, Structural investigation of monolayers prepared by deposition of (CH3S)(2) on the (111) face of single-crystal gold, J. Phys. Chem. B 106 (2002) 11771–11777.
[30] G. Bracco, G. Scoles, Study of the interaction potential between He and a self-assembled monolayer of decanethiol, J. Chem. Phys. 119 (2003) 6277–6281.
[31] D. Farias, K.H. Rieder, Atomic beam diffraction from solid surfaces, Rep. Prog. Phys. 61 (1998) 1575–1664.
[32] G. Comsa, B. Poelsema, The scattering of thermal he atoms at ordered and disordered surfaces, Appl. Phys. A-Mater. Sci. Process. 38 (1985) 153–160.
[33] G. Comsa, B. Poelsema, Scattering from disordered surfaces, in: G. Scoles (Ed.), Atomic and Molecular Beam Methods, Oxford University Press, 1992.
[34] B. Poelsema, R.L. Palmer, G. Mechtersheimer, G. Comsa, Helium scattering as a probe of the clean and adsorbate covered Pt(111) surface, Surf. Sci. 117 (1982) 60–66.
[35] M.F. Danisman, B. Ozkan, Simultaneous detection of surface coverage and structure of krypton films on gold by helium atom diffraction and quartz crystal microbalance techniques, Rev. Sci. Instrum. 82 (2011).
[36] E. Albayrak, M.F. Danışman, Helium diffraction study of low coverage phases of mercaptoundecanol and octadecanethiol self-assembled monolayers on Au(111) prepared by supersonic molecular beam deposition, J. Phys. Chem. C 117 (2013) 9801–9811.
[37] E. Mete, I. Demiroglu, E. Albayrak, G. Bracco, S. Elliatioglu, M.F. Danisman, Influence of steps on the tilting and adsorption dynamics of ordered pentacene films on vicinal Ag(111) surfaces, J. Phys. Chem. C 116 (2012) 19429–19433.
[38] D.J. Lavrich, S.M. Wetterer, S.L. Bernasek, G. Scoles, Physisorption and chemisorption of alkanethiols and alkyl sulfides on Au(111), J. Phys. Chem. B 102 (1998) 3456–3465.
[39] T. Hayashi, K. Wakamatsu, E. Ito, M. Hara, Effect of steric hindrance on desorption processes of alkanethiols on Au(111), J. Phys. Chem. C 113 (2009) 18795–18799.
[40] J. Noh, E. Ito, M. Hara, Self-assembled monolayers of benzenethiol and benzenemethanethiol on Au(111): influence of an alkyl spacer on the structure and thermal desorption behavior, J. Colloid Interface Sci. 342 (2010) 513–517.
[41] T. Shibue, T. Nakanishi, T. Matsuda, T. Asahi, T. Osaka, Thermal desorption high-resolution mass spectrometry of mixed self-assembled monolayers on gold, Langmuir 18 (2002) 1528–1534.
[42] F. Bensebaa, T.H. Ellis, A. Badia, R.B. Lennox, Probing the different phases of self-assembled monolayers on metal-surfaces - temperature-dependence of the CH stretching modes, J. Vac. Sci. Technol. A-Vac. Surf. Films 13 (1995) 1331–1336.
[43] R. Rousseau, V. De Renzi, R. Mazzarello, D. Marchetto, R. Biagi, S. Scandolo, U. del Pennino, Interfacial electrostatics of self-assembled monolayers of alkane thiolates on Au(111): work function modification and molecular level alignments, J. Phys. Chem. B 110 (2006) 10862–10872.